Virchows Arch (1997) 431:453–458

ORIGINAL ARTICLE

Tsutomu Matsushita · Tetsuro Takamatsu

Ischaemia-induced temporal expression of connexin43 in rat heart

Received: 4 April 1997 / Accepted: 19 June 1997

Abstract To investigate the regulation of cell-to-cell coupling in myocardial ischaemia, the three-dimensional expression of connexin43 (Cx43) during experimental ischaemia was examined using a confocal laser scanning microscope. After induction of myocardial infarction in rats, serial optical sections were obtained from the left ventricular myocardium at various times (3 h to 60 days after ligation). The expression of Cx43 was detected immunohistochemically with FITC-labelled anti-rat Cx43 antibody. Fluorescent dots of Cx43 remained along the intercalated disc and decreased in number around the infarct up to 12 h after ligation. Cx43-expression disappeared completely within 48 h after ligation. After day 4, and especially on days 8 and 15 after ligation, the edges of the cardiomyocytes bordering the infarcted area manifested numerous sarcoplasmic tentacles that reacted positively to anti-desmin antibody. Distinct expression of Cx43 was observed extensively on the tentacles, although no cardiomyocytes remained viable around them. By day 60 after ligation, atypical expression of Cx43 had disappeared. These findings suggest that ischaemia induces temporally abnormal expression of Cx43, which might be responsible for abnormal conduction around the infarct.

Key words Gap junction · Connexin43 · Rat heart · Ischaemia · Confocal laser scanning microscopy

Introduction

Arrhythmia is a common and potentially life-threatening complication of myocardial ischaemia and infarction. Abnormalities in conduction and propagation of electrical impulses stimulate cardiac contraction. Since electrophysiological studies have focused on the border zone of myocardial infarction as the site where slow conduction arises, the ischaemic or infarcted zone is presumed to be the major aetiological factor in those arrhythmias that involve circulating excitation and re-entry [4, 10, 22].

The calcium wave, a heterogeneous and abnormal rise of $[Ca^{2+}]_i$ during the condition of Ca^{2+} overload, initiates propagation from cardiomyocyte clusters to adjacent cells through gap junctions with a refractory period [20]. This phenomenon usually depends on conduction through gap junctions at intercalated discs. However, propagation of the calcium wave may occur at gap junctions abnormally expressed at sites other than the intercalated discs. If the calcium wave occurred in the remaining cardiomyocytes at the border zones of infarcts, on-site cell-to-cell coupling through gap junctions might be disturbed [8, 13, 14, 16, 18].

The gap junction, a type of cell-to-cell junction, is composed of low-resistance intercellular pathways and mediates electrical and metabolical coupling between adjacent cells. A gap junctional channel contains two abutting connexons aligned with one another so as to bridge the narrow gap between the adjacent membranes [1, 23]. Connexons are hexamers constructed of proteins called connexin [1, 23]. Of these, the major candidate in the cardiac gap junction in mammals is a 43-kDa protein called connexin43 (Cx43) [2]. In the mammalian ventricle, cell-to-cell plasma membrane interactions occur at the intercalated discs, and the gap junctions are organized in the intercalated discs to ensure orderly and synchronous communication.

To investigate the regulation of coupling in myocardial ischaemia, the present study examined 3-D and temporal expressions of Cx43, especially in the early phase, as a substitute for cardiac gap junctions in experimental infarction by coronary ligation in rats. Cardiomyocytes bordering the infarct showed many tentacle-like processes indicative of sarcoplasm later than day 4 after coronary ligation. Confocal images taken from areas opposite the infarct showed abnormal expression of Cx43 on sarcolemmae of numerous cardiomyocytes, especially on their tentacles, from day 4 to day 15 after ligation.

T. Matsushita · T. Takamatsu (✉)
Department of Pathology and Cell Regulation,
Kyoto Prefectural University of Medicine,
Kawaramachi-Hirokoji, Kamikyo-ku, Kyoto, 602 Japan
Tel.: (81) 75-251-5322, Fax: (81) 75-251-5353

Materials and methods

Myocardial infarction was induced in 50 young adult male Wistar rats (250 g) according to Ytrehus' method [25]. This study adhered to the standards detailed in "Principles of laboratory animal care" (NIH publication no. 85-23, revised 1985), and also to the specific university laws: "Rules and Regulations of the Animal Research, Kyoto Prefectural University of Medicine". Under isoflurane anaesthesia and ventilation with 100% oxygen, the pericardium of rats restrained in a supine position was exposed surgically by thoracotomy on the left side, between the 4th and 5th ribs. A 5-0 prolene suture on a tapered needle was looped around a branch of the left coronary artery for subsequent ligation (Fig. 1). In the sham-operated group, the ligature was not tightened. After closure of the chest incisions in layers, the rats were allowed a recovery period of not less than 3 h.

As a control, a rat anaesthetized with ether was subjected to coronary ligation for 3 h. Isoflurane is a volatile anesthetic similar to enflurane, which induces reversible gap junction closure [3].

Hearts excised under ether anaesthesia after coronary ligation at various times (3, 6, 12, 24, 48 h, 4, 8, 15, 30 and 60 days after ligation) were sectioned transversely across the infarct into two or three blocks. The tissue blocks were then fixed in 2% paraformaldehyde with 0.01 M phosphate-buffered saline (PBS, pH 7.4). After gradual infiltration with Tissue-Tek OCT compound (Miles, USA), the specimens were frozen in dry ice/acetone. Serial 20- and 3-μm-thick frozen sections were prepared and collected on silan-coated slides (Matsunami, Japan) with a cryostat microtome (Bright 5030 microtome, England). The 3-μm sections were stained with phosphotungstic acid haematoxylin (PTAH) stain for histological study, while the 20-μm thick sections were incubated with 0.03% azocarmin G (Chroma, Germany [21]) for 5 min. After washing in PBS containing 0.1% Triton X-100 for 15 min, the 20-μm thick sections were treated with 2% normal goat serum (Vector, USA) and incubated overnight at 4°C with monoclonal anti-rat Cx43 antibodies (1:500, anti-Cx43 sequence of amino acids 252–270 of rat Cx43, Chemicon, USA [1, 2, 9]) diluted from the saturated solution. The specimens were then rinsed with PBS and incubated further for 1 h with fluorescein isothiocyanate (FITC)-labelled goat anti-mouse IgG (1:300, Cappel/Organon Teknika, USA). In some sections, rabbit anti-desmin antibodies (1:40, Chemicon, USA) were used as a primary antibody instead of azocarmin G, and tetramethylrhodamine isothiocyanate (TRITC)-labelled goat anti-rabbit IgG (1:300, Dako, Denmark) was used as a secondary antibody [5]. Specimens were finally rinsed with PBS and mounted in Vectashield (Vector Laboratories, USA). The present study focused on the changes of Cx43 expression in and around the infarct site of middle layers of the left myocardial muscle, where cardiomyofibres were cut parallel to the longitudinal axis of cells (Fig. 1). All figures were transverse optical sections of the left myocardium in which the cardiomyocytes were sectioned longitudinally.

Immunohistochemical control experiments were performed using only the secondary antibodies without anti-Cx43 antibody in the presence of normal mouse serum.

The system for optical tomography [12, 17, 19, 24]) consisted of a scanning laser microscope (GB-100, Olympus, Japan), an image processor (Nexus 6000, Nexus, Japan) and a host computer (HP-9000, Hewlett-Packard, USA). An argon laser beam (wavelength 488 nm for FITC and azocarmin G signals and 514.5 nm for TRITC signal) was focused on a specimen through an objective lens (SPlanApo ×20, N.A. = 0.7, Olympus, Japan) or an oil immersion objective lens (SPlanApo ×60, N.A. = 1.4, Olympus, Japan). Fluorescent emissions passing through two dichroic mirrors (wavelength: 500 and 550 nm) and two barrier filters (IF535 and O590) were directed to a photomultiplier through a 30-μm pinhole. Fluorescence intensity data for image generation were transferred to the image processor (512 × 480 × 8 bits). Each confocal image was generated by eight integrations of a frame scan with double zooming. Optical sections of the myocardial cell layers were successively obtained by raising the sample stage at intervals of 0.35 μm by using a piezoelectric translator.

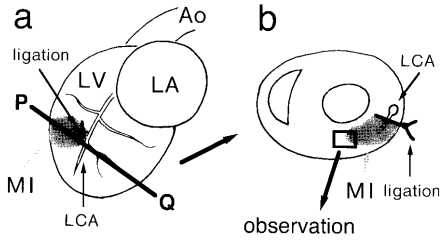

Fig. 1a, b Schematics illustrating the operation performed to induce experimental myocardial infarction in rats. **a** Coronary ligation induced myocardial infarction (*MI*). **b** Frozen sections containing infarcted areas were obtained by transverse section along *PQ* in **a** (*Ao* ascending aorta, *LA* left atrium, *LV* left ventricle)

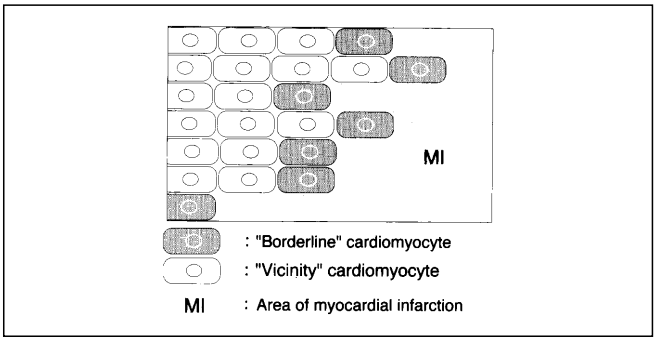

Fig. 2 Schematic representation of the "vicinity" and "borderline" cardiomyocytes. The latter displayed edges crossing the longitudinal axis bordering the area of myocardial infarction (*MI*), and the other edge extended to an adjacent cardiomyocyte with an intercalated disc. Furthermore, besides the borderline cells, vicinity cardiomyocytes were most probably affected by the ligation-induced ischaemia

Results

Red fluorescence of azocarmin G revealed clear striations in the sarcoplasm of heart muscle cells. Sequential

Fig. 3 Confocal images of the left ventricular myocardium at 6 h after ligation, stained with **a** azocarmin G and **b** FITC-labelled anti-Cx43 (connexin 43) antibody. Cx43 fluorescence between cardiomyocytes that exacerbated to contraction band necrosis was scattered around the sites where intercalated discs previously existed. ×20, *bar* 30 μm

Fig. 4 Confocal ventricular images of the infarct at 48 h after ligation, stained with **a** azocarmin G and **b** FITC-labelled anti-Cx43 antibody. Cx43 fluorescence was absent in the infarct zone (*arrowheads*) and the edges of borderline cardiomyocytes. In addition to partial red broken striations (**a**), most of the necrotic cardiomyocytes were thinly co-stained with green fluorescence. ×20, *bar* 30 μm

Fig. 5a A confocal ventricular image and **b** an extended-focus ventricular image with XZ and YZ sectioning images corresponding to the yellow lines on day 8 after coronary ligation. The infarct zone was on the *right*. **a** Borderline cardiomyocytes possessed many tentacles stained fluorescent red by azocarmin G. Green Cx43 fluorescence was dispersed extensively around the cell boundary (*arrowhead*). **b** Magnified version of the *boxed area* in **a**. Borderline cardiomyocytes possessed many tentacles extending to the infarcted area. Cx43 expression was scattered all over the cell surface, especially over the tentacles. **a** ×20, *bar* 30 μm, **b** ×60, *bar* 10 μm

Fig. 6 PTAH-stained ventricle on day 8 after ligation. Borderline cardiomyocytes possessed edges that were surrounded by only stromal cells and debris of necrotic cardiomyocytes. ×20

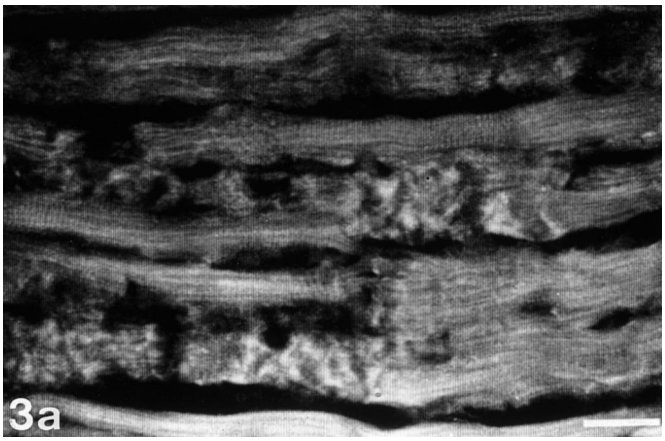
3a

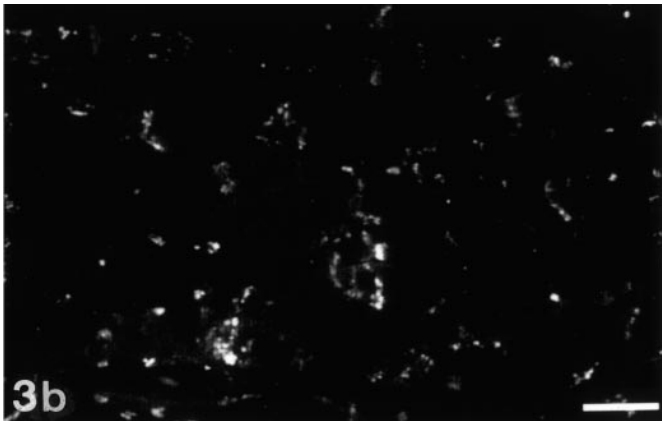
3b


4a

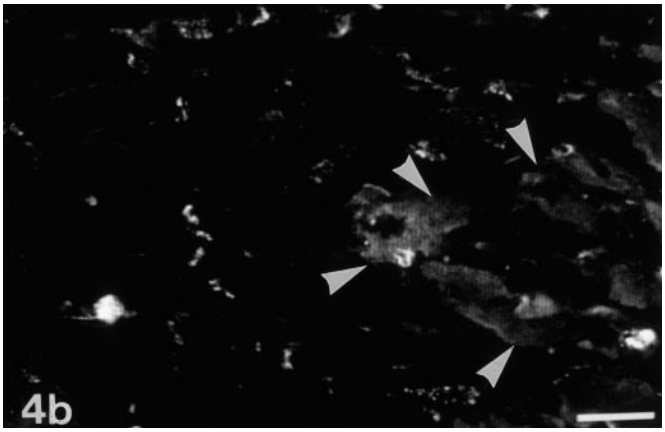
4b

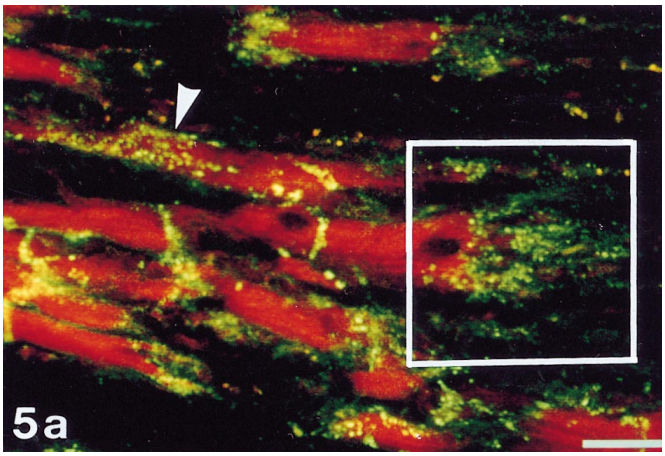
5a

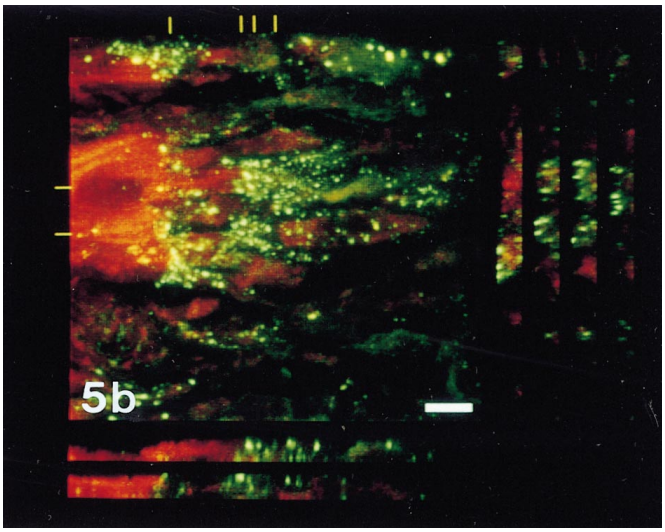
I
II
5b

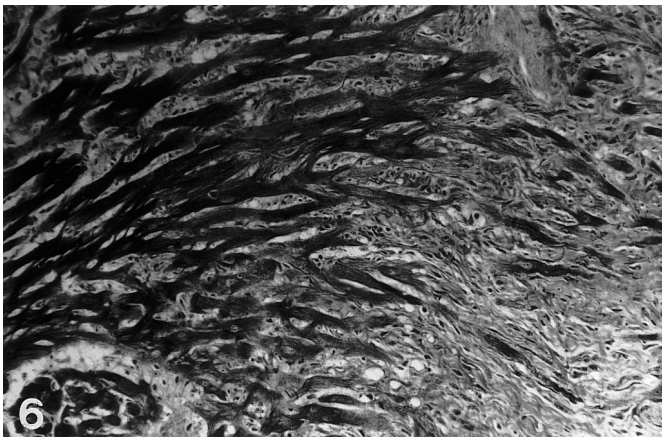
6

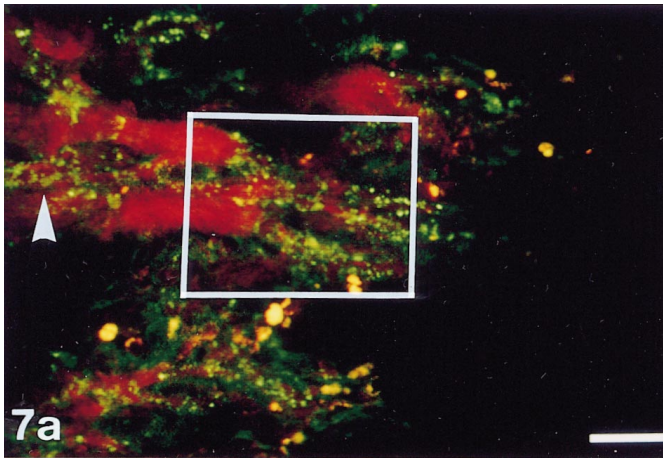

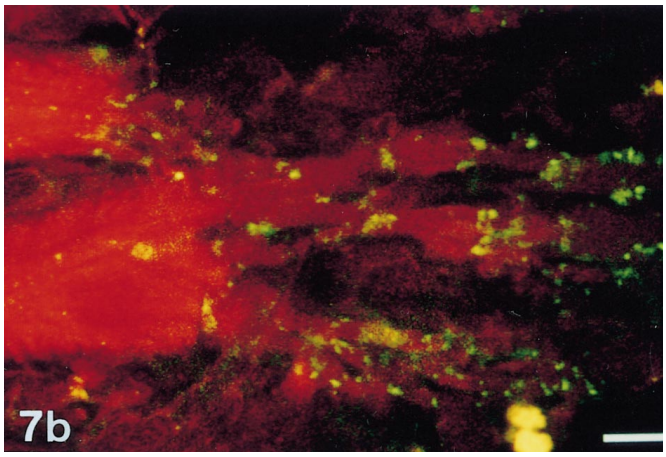

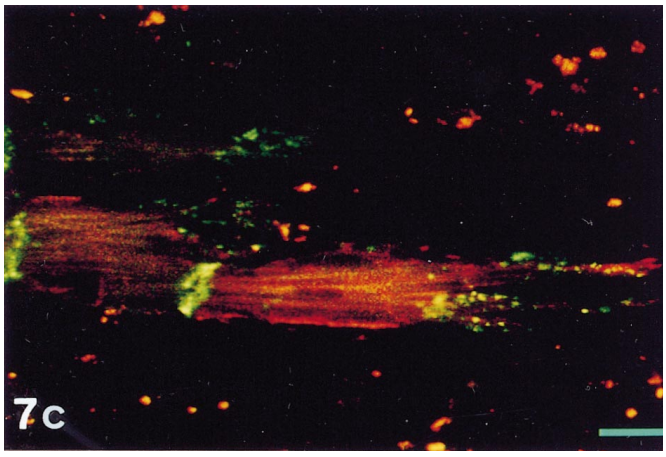

Fig. 7a–c Confocal images taken from the infarct border zone on day 15 after ligation. The infarct zone was on the *right*. **a**, **b** Cardiomyocytes were stained with azocarmin G. **c** Cardiomyocytes are immunostained by TRITC-labelled anti-desmin antibody. **a** Borderline cardiomyocytes facing the infarct possessed many tentacles, which had enlarged and lengthened compared with those seen on day 8 (Fig. 5). Cx43 expression was scattered around the tentacles. In the vicinity cardiomyocytes, fluorescent dots of Cx43 aligned with the lateral boundary along the long axis between neighbouring cardiomyocytes (*arrowhead*). **b** Magnified version of the *boxed area* in **a**. Distended long tentacles flourished and Cx43 fluorescence scattered all over the surface of tentacles. **c** TRITC fluorescence revealed clear striations of sarcoplasm of cardiomyocytes. Other cells were not identified by desmin fluorescence staining. The borderline cardiomyocyte displayed some tentacles similar to those stained by azocarmin G. Cx43 fluorescence was dispersed around the tentacles. **a**, **c** ×20, bar 30 μm, **b** ×60, *bar* 10 μm

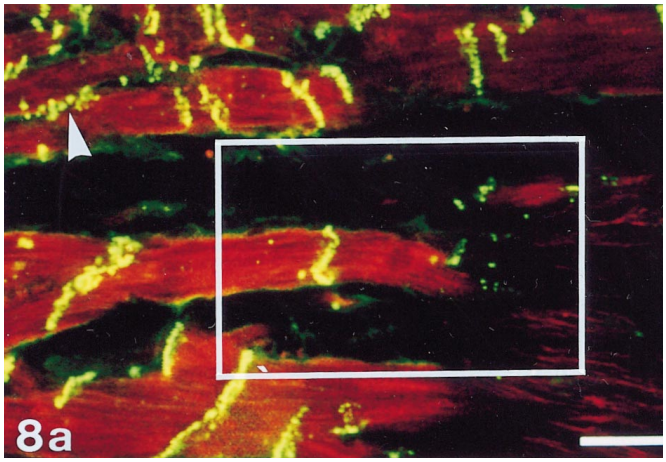

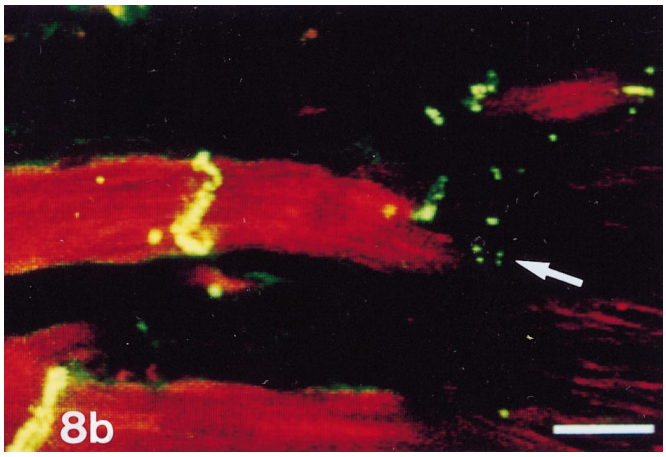

Fig. 8a, b Confocal images of the ventricle on day 60 after ligation. The infarct zone was on the *right*. **a** Fluorescent dots of Cx43 expressed along and between the long axes of neighbouring cardiomyocytes (*arrowhead*). **b** Magnified version of the *boxed area* in **a**. The borderline cardiomyocyte facing the infarct possessed large tentacles. The intensity of Cx43 distribution on the tentacles was attenuated compared with those visualized on days 8 and 15 after ligation (*arrow*). **a** ×20, *bar* 30 μm, **b** ×20, *bar* 15 μm

confocal images taken from 20-μm-thick sections revealed clear 3-D distribution of Cx43 as aggregates of green fluorescent domains along the intercalated discs between cardiomyocytes, with occasional alignment along the side of normal left ventricular “working” cardiomyocytes of sham-operated rats.

In the following description, we use the terms “borderline” and “vicinity” to discriminate cells located differently with reference to the infarct (Fig. 2). A “borderline” cardiomyocyte is one that had its lateral boundary along the short axis adjacent to the infarct with its opposite boundary adjoining an adjacent cardiomyocyte with an intercalated disk; “vicinity” is applied to the neighbouring myocardial tissues surrounding the “borderline” cardiomyocytes in areas opposite to the myocardial infarct. The vicinity cardiomyocytes were probably affected by the ischaemia.

At 3 h after ligation, infarcted cardiomyocytes could be clearly identified by the broken striations revealed by dimmer azocarmin G fluorescence and co-stained thinly with green fluorescence over the broken striations. Cx43 expression in infarcted areas was aligned along the intercalated discs although the fluorescent count and intensity were attenuated. There was no difference in the expression of Cx43 in rat hearts between isoflurane and ether anaesthesia.

At 6 h after ligation, contraction band necrosis with broken striations was distinctly displayed (Fig. 3). Although some necrotic cardiomyocytes demonstrated regular Cx43 fluorescence along the intercalated discs, other necrotic cardiomyocytes manifested the necrosis as scattered Cx43 fluorescence dotted around the intercalated discs (Fig. 3).

By 12 h after ligation, expression of Cx43 in the cardiomyocytes with infarction remained visible at the intercalated discs, although the count and intensity decreased with time. By 24–48 h after ligation, Cx43 fluorescence disappeared in the infarct zone and at the edge of borderline cardiomyocytes facing the infarct (Fig. 4). Most of the necrotic cardiomyocytes were co-stained with FITC accompanied by partial red broken striations. In the vicinity cardiomyocytes, Cx43 fluorescence prevailed mainly at the intercalated discs.

Azocarmin G fluorescence facilitated discrimination of cardiomyocytes from other cell populations such as fibroblasts, because the latter displayed only weak red fluorescence in comparison with the typical intensity of cardiomyocytes.

On day 4, the edges along the short axis of borderline cardiomyocytes facing the infarct began to mould into a round patch. Some borderline cardiomyocytes extended small but fine cytoplasmic tentacles toward the infarct. In addition, many Cx43 fluorescent spots were distributed extensively around the cell surfaces on the cell border along the short axis of borderline cardiomyocytes, with spindle- or tentacle-like structures.

On day 8, 3-D reconstructed images along the XZ and YZ axes illustrated numerous borderline cardiomyocytes with longer tentacles dotted with many fluorescent spots of Cx43 around the tentacles in a dispersed fashion (Fig. 5a, b). These fluorescent spots were smaller than those observed at the intercalated discs between normal cardiomyocytes. There was an absence of red fluorescence of other cardiomyocytes around the tentacles. PTAH staining indicated that only stromal cells and necrotic ghosts of cardiomyocytes surrounded the tentacles (Fig. 6). There were no green fluorescent spots in the infarct zone. Cardiomyocytes one cardiomyocyte away from the infarct site showed no changes in Cx43 expression along the intercalated discs, although dispersed Cx43 expression at the lateral boundary along the long axis was seen.

On day 15, the tentacles enlarged and lengthened, accompanied by Cx43 fluorescence dispersed around the tentacles in a manner similar to the distribution on day 8 after ligation (Fig. 7a, b). Immunofluorescence illuminated by TRITC-labelled anti-desmin antibody instead of azocarmin G, demarcated red signals of striations of cardiomyocytes without direct contact with other cardiomyocytes (Fig. 7c). The borderline cardiomyocyte had some tentacles illuminated by TRITC identical to those revealed by azocarmin G fluorescence. In the vicinity cardiomyocytes, fluorescent dots of Cx43 had aligned with the lateral boundary along the long axis between neighbouring cardiomyocytes (Fig. 7a).

Although thickened and extended tentacles of borderline cardiomyocytes were observed on days 30 and 60, there was a decrease in number. The dispersion of Cx43 fluorescence around the tentacles was attenuated, demonstrating a lower intensity than that recorded on days 8 and 15 after ligation (Fig. 8). However, Cx43 expression aligned at the lateral boundary along the long axis of vicinity cardiomyocytes showed an intensity and a count similar to those observed on day 15 after ligation (Fig. 8a).

Discussion

The combination of azocarmin G staining with confocal laser scanning microscopy rendered visualization of cardiomyocytes possible with exceptional clarity through a substantial depth of rat ischaemic heart tissue. Azocarmin G stained sarcoplasmic cardiomyocytes and tentacles in a similar manner to immunostaining by TRITC-labelled anti-desmin antibodies; the latter confirmed that the antibodies reacted with only muscle cells [5]. The patterns of immunostained Cx43 distribution in normal cardiomyocytes accorded with the classic organization of gap junctions at cardiac intercalated disks [6, 7, 9, 15]. Detailed 3-D observations established characteristic changes to borderline cardiomyocytes with many tentacles of various lengths coursing toward the infarct. The tentacles fanned out in search of other cells. Although comparisons with the neighbouring PTAH-stained sections were attempted, many stromal cells devoid of cardiomyocytes were distributed around the tentacles.

Ultrastructural observation of the vicinity cardiomyocytes revealed cell processes from one vicinity cardiomyocyte interacting with the main body of a neighbouring cardiomyocyte [16, 18]. In our study, many large tentacles from a cardiomyocyte facing stromal cells and necrotic ghosts of cardiomyocytes in the infarcted area did not face the other cardiomyocytes. The location of these large tentacles coincided well with that of the intercalated disc. This suggests that an intercalated disc of a borderline cardiomyocyte induced by the ligation changed its form, to mould into tentacle-like structures. Cx43 expression on the tentacles might not indicate the redistribution of the protein previously located at the intercalated disc since Cx43 fluorescence had formerly disappeared on the disc at 24–48 h after ligation. Cx43 expression around the tentacles was less intense than that of normal intercalated disks, implying that the connexons were newly constructed.

The anti-Cx43 antibody used in the present study detected only the existence of Cx43-protein. This would thus recognize not only the presence of a complete gap junction with direct connections between the cells, but also the presence of hemichannels without connections. The functional connection between cardiomyocytes and connective tissues through the gap junction is unclear. Borderline cardiomyocytes might come in contact with neighbouring cells to transmit signals and thereby complete uniform cardiac contraction. As such, those cardiomyocytes with extended tentacles and expressed Cx43 may search for nearby cells in the same way as sea anemones sway their tentacles to catch fish.

After day 8 after ligation, fluorescent spots of Cx43 were observed dotted extensively over the longitudinal sides of cardiomyocytes bordering the infarct. This change has been described in the canine subacute to chronic phase and in human chronic myocardial infarction [8, 11, 13, 14, 16, 18]. Our study further demonstrated that the change occurred in the early phase of myocardial infarction. On day 60 after ligation, distribution of Cx43 around the tentacles became sparse. In human borderline cardiomyocytes facing the healed infarct, Cx43 expression was not observed [18]. Even in rat myocardial infarcts, Cx43 expression around the tentacles may diminish with time.

Cx43 expression symbolized not only the presence of a complete gap junction where direct cell–cell connections prevailed but also the presence of a hemichannel without any contact. Thus, Cx43 expression using monoclonal anti-Cx43 antibody may represent the existence of newly formed Cx43, although further experiments are necessary to confirm such a finding.

Acknowledgements The authors thank Dr. Kouichi Kawamura, Department of Pathology, Akita University School of Medicine for sharing his expertise in surgical induction of ischemia. This work is supported by a Grant-in-Aid for Scientific Research from The Ministry of Education, Science, Sports and Culture of Japan (T.T. 07457064). Thanks are due to Dr. Anthony Foong for reading the manuscript.

References

1. Bennett MVL, Barrio LC, Bargiello TA, Spray DC, Hertzberg E, Saez JC (1991) Gap junctions: new tools, new answers, new questions. Neuron 6:305–320
2. Beyer EC, Paul DL, Goodenough DA (1987) Connexin43: a protein from rat heart homologous to a gap junction protein from liver. J Cell Biol 105:2621–2629
3. Burt M, Spray DC (1989) Volatile anesthetics block intercellular communication between neonatal rat myocardial cells. Circ Res 65:829–837
4. Dillon SM, Allessie MA, Ursell PC, Wit AL (1988) Influences of anisotropic tissue structure on reentrant circuits in the epicardial border zone of subacute canine infarcts. Circ Res 63:182–206
5. Garcia-Martines V, Hurle JM (1986) Cell shape and cytoskeletal organization of endothelial cells of the semilunar heart valves in the developing chick. Anat Embryol 174:83–89
6. Gourdie RG, Green CR, Severs NJ (1991) Gap junction distribution in adult mammalian myocardium revealed by an anti-peptide antibody and laser scanning confocal microscopy. J Cell Sci 99:41–55
7. Gourdie RG, Green CR, Severs NJ, Thompson RP (1992) Immunolabeling patterns of gap junction connexins in the developing and mature rat heart. Anat Embryol 185:363–378
8. Green CR, Severs NJ (1993) Distribution and role of gap junctions in normal myocardium and human ischaemic heart disease. Histochemistry 99:105–120
9. Kanter HL, Laing JG, Beau SL, Beyer EC, Saffitz JE (1993) Distinct patterns of connexin expression in canine Purkinje fibers and ventricular muscle. Circ Res 72:1124–1131
10. Kleber AG (1987) Review. Conduction of the impulse in the ischemic myocardium – implications for malignant ventricular arrhythmias. Experientia 43:1056–1061
11. Luke RA, Saffitz JE (1991) Remodeling of ventricular conduction pathways in healed canine infarct border zones. J Clin Invest 87:1594–1602
12. Minamikawa T, Takamatsu T, Fujita S (1991) Application of laser microtomography to in situ three-dimensional subcellular morphology. Acta Histochem Cytochem 24:55–60
13. Peters NS (1995) Myocardial gap junction organization in ischemia and infarction. Microscopy Res Techn 31:375–386
14. Peters NS, Green CR, Poole-Wilson PA, Severs NJ (1995) Review: cardiac arrhythmogenesis and the gap junction. J Mol Cell Cardiol 27:37–44
15. Severs NJ (1990) The cardiac gap junction and intercalated disc. Int J Cardiol 26:137–173
16. Severs NJ (1994) Pathophysiology of gap junctions in heart disease. J Cardiovasc Electrophysiol 5:462–475
17. Shiraishi I, Takamatsu T, Fujita S (1995) Three-dimensional observation with a confocal scanning laser microscope of fibronectin immunolabeling during cardiac looping in the chick embryo. Anat Embryol 191:183–189
18. Smith JH, Green CR, Peters NS, Rothery S, Severs NJ (1991) Altered patterns of gap junction distribution in ischemic heart disease. Am J Pathol 139:801–821
19. Takamatsu T, Fujita S (1988) Confocal laser scanning microscopy and its three-dimensional application. J Microsc 149:167–174
20. Takamatsu T, Fujita S (1994) Use of confocal laser scanning microscope in cytochemistry. Acta Histochem Cytochem 27:495–498
21. Takamatsu T, Nakanishi K, Fukuda M, Fujita S (1981) Cytofluorometry on cells isolated from paraffin sections after blocking of the background fluorescence by azocarmin G. Histochemistry 71:161–170
22. Ursell PC, Gardner PI, Albata A, Fenoglio JJ, Wit AL (1985) Structural and electrophysiological changes in the epicardial border zone of canine myocardial infarcts during infarct healing. Circ Res 56:436–451
23. Warner AE (1988) The gap junction. J Cell Sci 89:1–7
24. Yasui H, Takamatsu T, Fujita S (1994) “Varicoid change” of bile canaliculi in rat liver at an early phase of ischaemia-reperfusion injury. Virchows Arch 425:505–512
25. Ytrehus K, Liu Y,Tsuchida A, Miura T, Liu GS, Yang X, Herbert D, Cohen MV, Downey JM (1994) Rat and rabbit heart infarction: effects of anesthesia, perfusate, risk zone, and method of infarct sizing. Am J Physiol 267:H2383–H2390